

## Formation of Nanobubbles at the Water-Graphite Interface

Prabhakar Misra<sup>1</sup>, Silvina M. Gatica<sup>1</sup>, and Obafemi Otelaja<sup>2</sup>

### Summary

Nanobubbles form either spontaneously or by induction at the surface of certain solids immersed in a liquid. Atomic Force Microscopy observations have confirmed their formation. Such bubbles have sizes in the range 10-100 nm and have important ramifications for properties of interfaces and could be responsible for long-range hydrophobic attractive forces. In addition, as a potential application, the use of nanobubbles – in tandem with ultrasound – has been proposed for the treatment of strokes. Formation of nanobubbles at the water-graphite interface influences the adsorption of nanoparticles and the corresponding wetting properties. An important parameter relevant to the stability of the nanobubble is the contact angle, which in turn, depends on the surface tensions of the substrate, liquid and vapor involved at the water-graphite interface through the Young's equation. We have developed a quantitative model that incorporates the attraction of the substrate and allows the determination of the contact angle as a function of temperature. Our computed results compare favorably with the experimental data available in the open literature.

### Introduction

Nanobubbles are tiny gas bubbles (usually of an atmospheric gas) found on the surfaces of some liquids. They are found at the liquid/solid interface and are fairly stable. Although the existence of nanobubbles has been debated for some time, Atomic Force Microscopy (AFM) studies have confirmed their formation [1]. The existence of nanobubbles at water/solid interfaces has been proposed to explain long-range hydrophobic attractive forces in surface interactions. The current interest in the study of nanobubbles has potential ramifications for design of microdevices and in manufacturing relating to nanostructures [2]. In addition, nanobubbles—in conjunction with ultrasound—have been proposed for the treatment of strokes [3]. Generally, an *a priori* knowledge regarding the presence of nanobubbles is very important as they can cause unforeseen forces in systems involving liquid-surface interactions.

An important parameter pertinent to the stability of the bubble is the contact angle at the liquid-vapor-solid interface, which in turn depends on the surface tensions of the substrate, liquid and vapor involved through the Young's equation [4]:

$$\sigma_{gs} = \sigma_{ls} + \sigma_{lg} \cos(\theta) \quad . \quad (1)$$

---

<sup>1</sup>Department of Physics and Astronomy, Howard University, Washington, DC 20059, USA

<sup>2</sup>Department of Electrical and Computer Engineering, Howard University, Washington, DC 20059, USA

In Eqn. (1),  $\sigma_{gs}$ ,  $\sigma_{ls}$ , and  $\sigma_{lg}$  are the gas-solid, liquid-solid, and liquid-gas surface tensions, respectively, and  $\theta$  is the angle formed between the liquid and solid surfaces (see Fig. 1), i.e.  $\theta = 0$  corresponds to a complete wetting situation, or a perfect spherical bubble. The latter condition is achieved when the surface tensions fulfill the particular relation:

$$\sigma_{gs} = \sigma_{ls} + \sigma_{lg} \quad (2)$$

The case of  $\theta > 0$  corresponds to non-wetting or “partial wetting”, and a bubble with a flat surface supported by the substrate. The value of the contact angle is determined by a delicate competition between cohesive and adhesive forces. This description in terms of macroscopic surface tensions applies only at saturated vapor pressure (svp), where the strength of the attraction of the substrate can cause the fluid to spread over the surface rather than condense into droplets. The change in the contact angle  $\theta$  from a nonzero to zero value indicates the occurrence of a wetting transition. Since the surface tension depends strongly on the temperature of the interface, when a fluid does not wet a particular surface, a wetting transition may occur at a higher temperature  $T_w$ . Such phase transitions were first observed for He, Ne and H<sub>2</sub> on alkali metal surfaces [5]. For the water-graphite interface, a transition has been predicted at a temperature  $T_w \sim 350\text{-}500$  K [6].

In this paper, we determine the contact angle as a function of temperature for a nanobubble formed at the water-graphite interface and based on Eqn. (4).

### Description of the model

A simple model for the liquid-solid surface tension,  $\sigma_{ls}$ , has been presented by Cheng et al. [7]:

$$\sigma_{ls} - \sigma_{gs} = \sigma_{lg} + \rho \int dz V(z) \quad (3)$$

where  $\rho$  is the adsorbate's density and  $V(z)$  is the adsorption potential.

This simple model makes a drastic assumption that the liquid-solid surface tension,  $\sigma_{ls}$ , includes two contributions, namely the free energy associated with terminating the liquid ( $\sigma_{lg}$ ) and the liquid-surface interaction energy. The domain of integration extends between the minimum in the adsorption potential at ( $z = z_{\min}$ ) and infinity. With this model, we incorporate the attraction of the substrate to calculate the contact angles, from Eqns. (1) and (3). It is important to note that the dependence of the contact angle on temperature appears implicitly in  $\sigma_{lg}$  and  $\rho$ .

For the substrate potential, we use the continuous approximation, an extensively used model for treating wetting and adsorption problems that integrates the interaction between atoms in the substrate and adsorbate over a semi-infinite solid to yield:

$$V(z) = \frac{4C_3^3}{27D^2z^9} - \frac{C_3}{z^3} \quad (4)$$

Here  $C_3$ , the asymptotic van der Waals coefficient, and  $D$ , the well depth of the adsorption potential, are characteristics of the surface material. Such a 3-9 potential is analogous to the Lennard-Jones 6-12 interatomic potential. Inserting Eqn. (5) into Eqn. (4), with  $z_{\min} = [2C_3/(3D)]^{1/3}$ , the following is obtained for the integration in the right hand side of Eqn. (3):

$$I = \frac{11}{24} \left(\frac{3}{2}\right)^{2/3} (C_3 D^2)^{1/3} \quad (5)$$

where  $I = -\int dzV(z)$ . Eqns. (3)-(5) above result from a combination of the simple model for the surface tension,  $\sigma_{ls}$ , with the 3-9 model potential.

### The Water – Graphite Interface

In Fig. 1, a top level representation of the water-graphite interface is depicted. From the Eqns. (1)-(5) above, we can derive the contact angle at the water-graphite interface:

$$\theta = \cos^{-1}\left(-1 + \frac{\rho}{\sigma_{lg}}I\right), \quad (6)$$

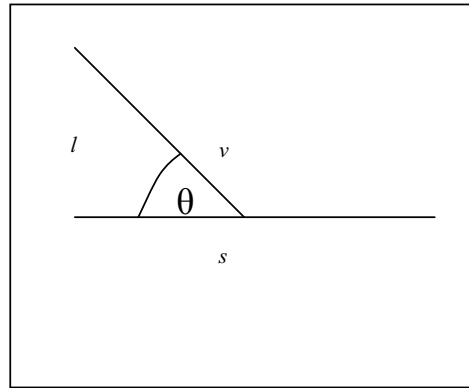


Figure 1: A representation of the Water-Air-Graphite Interface,  $s = \text{graphite}$ ,  $l = \text{water}$ , and  $v = \text{water vapor (nanobubble)}$ .

The values of the parameters associated with the substrate potential, although well-known for many gas/surface combinations, were recently estimated to be  $C_3 = 1075 \text{ meV } \text{\AA}^3$  and  $D = 100 \text{ meV}$  for water-graphite [6]. The dispersion coefficient  $C_3$  has two independent contributions. The first one comes from the interaction between the water molecule's dipole moment and its image in the dielectric substrate. The second contribution is due to the coupled dipolar charge fluctuations on the water molecule and those of graphite. The well-depth  $D$  was estimated in [6] by comparison with the Zhao and Johnson potential [8]. We used these values and the data on the density and surface tension of water – air,  $\sigma_{lg}$ , at various temperatures [9] to determine the contact angles summarized in Table 1 below.

Table 1: Contact angle determination as a function of temperature, using appropriate values for the surface tension and density, and employing Eqn. (6).

Temp (K)	$\sigma$ (lg) (N/m)	$\rho$ (mol/l)	$\sigma/\rho$ (N.m <sup>2</sup> /mol)	C3 (N.m <sup>4</sup> /mol)	D (N.m/mol)	I (N.m <sup>2</sup> /mol)	$\cos(\theta)$	$\theta$ (deg)
273.16	0.07565	55.5	1.3631E-06	1.037E-25	9647.24	1.3E-6	-0.06186	93.546719
275.03	0.07565	55.5	1.3629E-06	1.037E-25	9647.24	1.3E-6	-0.06178	93.541977
278.16	0.07494	55.5	1.3502E-06	1.037E-25	9647.24	1.3E-6	-0.05291	93.032719
283.16	0.07422	55.49	1.3376E-06	1.037E-25	9647.24	1.3E-6	-0.04398	92.520521
510.58	0.02899	45.35	6.3938E-07	1.037E-25	9647.24	1.3E-6	0.999965	0.4769158

## Results and Conclusions

We have used the simple model given above to determine the contact angles at the water-air-graphite interface. The results of the calculations are summarized in Table 1. In addition, by plotting the contact angles at various temperatures (as illustrated in Fig. 2), we can conclude that  $T_w$  for the water-graphite interface is approximately 510.58 K, as the contact angle at this temperature approaches zero.

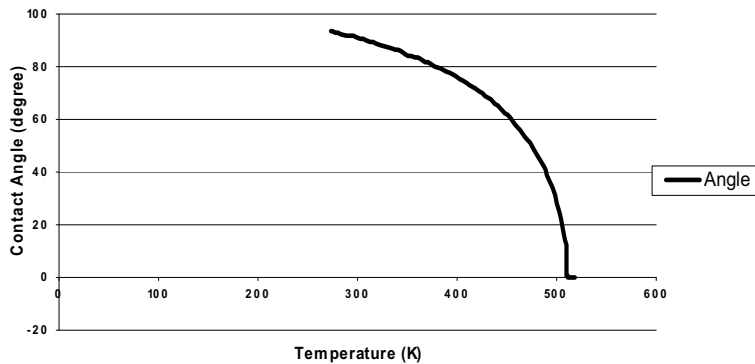


Figure 2: A plot of contact angle versus temperature for the water-air-graphite interface.



Figure 3: Schematic representation of the nanobubble for  $T \sim 500\text{K}$  (left) and  $T \sim$  room temperature (right).

As we see from the results displayed in Fig. 2 and Table 1, at  $T \approx 500\text{K}$  the contact angle drops abruptly to a value close to zero, due to the supremacy of the attraction of graphite over the cohesive forces. In this situation, the nanobubble will have a more or less spherical shape (as shown in Fig. 3). For lower temperatures, the cohesive forces prevail, forming a semispherical bubble supported by the surface (cf. Fig. 3). The precise shape and stability of the nanobubbles will have to be determined by minimization of the grand potential energy.

### References

1. Zhang, X.H.; Li, G.; Maeda, N.; Hu, J. (2006): "Removal of Induced Nanobubbles from Water/Graphite Interfaces by Partial Degassing", *Langmuir*, Vol. 22, pp. 9238-9243.
2. Fan, Y.W.; Wang, R.Z. (2005): *Adv. Mater.*, Vol. 17, p. 2384.
3. Unger, E.C. (2006): "Treatment of ischemic stroke with nanobubbles and ultrasound", *Journal of the Acoustical Society of America*, Vol. 119, No. 5, p. 3437.
4. Rowlinson, S.; Widom, B.(1989): *Molecular theory of capillarity*, Clarendon, Oxford.
5. Ross, D.; Tabor, P.; Rutledge, J.E. (1995): *Phys. Rev. Lett.* Vol. 74, pp. 4483-4486.
6. Gatica, S.M.; Johnson, J.K.; Zhao, X.C.; Cole, M.W. (2004): *J. Phys. Chem. B*, Vol. 108, pp. 11704-11708.
7. Cheng, E.; Cole, M.; Saam, W.F.; Treiner, J. (1991): *Phys. Rev. Lett.*, Vol. 67, pp. 1007-1010.
8. Zhao, X.C.; Johnson, J.K. (2005): *Mol. Sim*, Vol. 31, p. 1.
9. Data from NIST Standard Reference Database 69 (March 2003); Release: *NIST Chemistry WebBook*.

